Geomicrobiology Journal
Publication details, including instructions for authors and subscription information:
http://www.tandfonline.com/loi/ugmb20

Environmental Factors Affect Magnetite Magnetosome Synthesis in Magnetospirillum magneticum AMB-1: Implications for Biologically Controlled Mineralization

Jinhua Li [a b] & Yongxin Pan [a b]

[a] Bio-geomagnetism Group, Paleomagnetism and Geochronology Laboratory, Key Laboratory of Earth's Deep Interior, Institute of Geology and Geophysics, Chinese Academy of Sciences, Beijing, China

[b] France-China Bio-Mineralization and Nano-Structures Laboratory, Chinese Academy of Sciences, Beijing, China

Available online: 08 Feb 2012

To cite this article: Jinhua Li & Yongxin Pan (2012): Environmental Factors Affect Magnetite Magnetosome Synthesis in Magnetospirillum magneticum AMB-1: Implications for Biologically Controlled Mineralization, Geomicrobiology Journal, 29:4, 362-373

To link to this article: http://dx.doi.org/10.1080/01490451.2011.565401

Geomicrobiology Journal, 29:362–373, 2012

ISSN: 0149-0451 print / 1521-0529 online
DOI: 10.1080/01490451.2011.565401

Taylor & Francis
Taylor & Francis Group

Environmental Factors Affect Magnetite Magnetosome Synthesis in *Magnetospirillum magneticum* AMB-1: Implications for Biologically Controlled Mineralization

Jinhua Li[1,2] and Yongxin Pan[1,2]

[1]*Bio-geomagnetism Group, Paleomagnetism and Geochronology Laboratory, Key Laboratory of Earth's Deep Interior, Institute of Geology and Geophysics, Chinese Academy of Sciences, Beijing, China*
[2]*France-China Bio-Mineralization and Nano-Structures Laboratory, Chinese Academy of Sciences, Beijing, China*

It is widely believed that magnetotactic bacteria (MTB) form membrane-enveloped magnetite crystals (magnetosomes) under strict genetic control. In this study, the *Magnetospirillum magneticum* strain AMB-1 was cultured in the same growth medium, but under four different growth conditions: Anaerobic static, aerobic static, aerobic 80-rpm rotating, and aerobic 120-rpm rotating to investigate possible environmental influences on magnetite magnetosome formation. Integrated analyses, using transmission electron microscopy, X-ray diffraction and rock magnetism, indicate that, from the anaerobic static to aerobic 120-rpm rotating culture, the formed magnetite magnetosomes became more equidimensional, smaller in grain size, and higher in crystal twinning frequency. Magnetic properties of magnetite magnetosomes such as coercivity, remanence coercivity, remanence ratio and Verwey transition temperature systematically decreased from 22.0 mT to 5.2 mT, 31.3 mT to 9.3 mT, 0.45 to 0.31, and 108 K to 98 K, respectively. Comparison of additional anaerobic 120-rpm rotating cultures with anaerobic static cultures showed that the effect of rotating, at least up to 120 rpm, on the cell growth and magnetite magnetosome formation is weak and negligible. Given that all samples were prepared and measured in the same way, the changes in physical and magnetic properties indicate that environmental factors (oxygen) affected the biomineralization of magnetite magnetosomes in magnetotactic bacteria, which supports the previous findings. In all experiments, only magnetite with the geometry of truncated octahedron was formed within magnetosomes, which suggests that the mineral phase and crystal habit remain to be genetically controlled. These results also imply the physical and magnetic properties of magnetite magnetosomes may, to some extent, reflect the external growth environments.

Keywords magnetotactic bacteria, *M. magneticum* AMB-1, environmental factor, biologically controlled mineralization, rock magnetism

INTRODUCTION

Biomineralization is a process by which living organisms mediate the deposition of minerals. Based on the pathway, biomineralization can be distinguished into biologically induced mineralization (BIM) and biologically controlled mineralization (BCM) (Bazylinski et al. 2007; Edwards and Bazylinski 2008). In BCM minerals precipitate intracellularly on, or within specific organic matrices or vesicles, which allows the organism exert strict biological control over the biomineralization process.

Consequently, BCM products generally have perfect crystallography, consistent and specific morphologies, narrow particle size distributions, chemical purity and highly-ordered structures (Bazylinski et al. 2007). Magnetotactic bacteria (MTB) have the ability to synthesize intracellular, nanometer-sized, single domain (SD) magnetite (Fe_3O_4), or greigite (Fe_3S_4) crystals or both in organelles known as magnetosomes (Faivre and Schüler 2008). Magnetosome is widely considered as a model system for understanding the BCM process in organisms (Bazylinski et al. 2007; Pósfai and Dunin-Borkowski 2009). In view of geological records, fossil magnetosomes (also called magnetofossils) are considered as potential biomarkers in the search for early terrestrial and extraterrestrial life, proxies for reconstructing paleoenvironments, and important carriers of magnetic remanence in sedimentary rocks (Hesse 1994; Yamazaki and Kawahata 1998;

Received 22 October 2010; accepted 17 February 2011.
We thank Xin'an Yang, Nicolas Menguy and Lei Sun for assistance with TEM observations, Wei Lin and Qingsong Liu for constructive discussions, Greig. A. Paterson and Zach Oestreicher for improving the English. We thank Dr. B. Ghiorse and two anonymous reviewers for their constructive comments that have significantly improved this paper. This work was supported by NSFC grants (40821091, 41004024) and the CAS/SAFEA international Partnership Program for Creative Research Teams (KZCX2-YW-T10). J.H.L. thanks support from the China Postdoctoral Science Foundation. Y.X.P. thanks support from the CAS '100' Talents Program.

Address correspondence to Y. X. Pan, Institute of Geology and Geophysics, Chinese Academy of Sciences, 19 BeiTuChengXi Road, Beijing 100029. E-mail: yxpan@mail.iggcas.ac.cn

Pan et al. 2005a; Kopp and Kirschvink 2008; Jimenez-Lopez et al. 2010).

The synthesis of magnetite magnetosomes is achieved by a process of strict genetic control, which produces perfectly crystallized and highly ordered crystals with species-specific morphologies and sizes (Schüler 2008). Experiments on cultivated MTB strains have also demonstrated that the formation of magnetosomes can be affected by environmental factors (Blakemore et al. 1985; Faivre et al. 2008; Popa et al. 2009). For instance, Blakemore et al. (1985) first examined the effect of oxygen on the amount of magnetite magnetosomes within *Magnetospirillum magnetotacticum* MS-1 and proposed magnetofossils as a retrospective indicator of microaerobic environment. Faivre et al. (2008) found that the rates of Fe uptake influence the crystal-size distribution, aspect ratio, and morphology of magnetite magnetosomes in *Magnetospirillum gryphiswaldense* strain MSR-1. Popa et al. (2009) found that the cells of *Magnetospirillum magneticum* strain AMB-1 produced predominantly dwarfed magnetite magnetosomes in a 150 rpm-stirred culture containing 45 μM initial oxygen in the medium. However, systematic studies on the influence of environmental factors on magnetite magnetosome formation are still sparse. Such studies are essential in revealing the process of magnetite magnetosome biomineralization, as well as to gain a better understanding of the significance of magnetofossils as a proxy for paleoenvironments.

Magnetospirillum magneticum strain AMB-1, which was originally isolated in pure culture by Mutsunaga and his coworkers from freshwater sediment in Tokyo, Japan, has served as a model organism for MTB studies (Matsunaga et al. 1991; Matsunaga et al. 2005). AMB-1 is a facultative anaerobic with the capability of growing under a wide range of oxygen conditions. In the present study, we tested the effects of different growth conditions on magnetite magnetosome biomineralization by culturing AMB-1 in the same growth medium, but under four different growth conditions. Mineralogy, crystallography, and magnetic properties of magnetosomal magnetites were analyzed using transmission electron microscopy (TEM), X-ray diffraction (XRD) and rock magnetic methods. We found that the magnetosomal magnetites synthesized in AMB-1 under four growth conditions are different.

MATERIALS AND METHODS

Cell Culture and Sample Preparation

M. magneticum strain AMB-1 (ATCC700264) was used in this study. Non-magnetic cells were obtained by growing AMB-1 strains in iron-starved medium as described by Li et al. (2009). These non-magnetic cells of AMB-1 were then cultured in an enriched magnetic spirillum growth medium (EMSGM) with the addition of 60 μM ferric quinate. The starting cell density after inoculation was $\sim 5.0 \times 10^6$ cells/ml. Growth experiments were carried out with cells cultured at 26°C in 500 ml triangular flasks each containing 500 ml of culture medium. The flasks were sealed with 8 layers of gauze to prevent contamination, but allow for free gas exchange with the external environment.

The anaerobic static (ANS) experiment was carried out in an anaerobic glove box (ShangHai CIMO Medical Instrument Co., Ltd., China), which allowed the oxygen concentration to be reduced to lower than 0.02% (V/V). The aerobic static (AS) experiment was carried out in a static incubator, and the aerobic 80-rpm rotating (A80), and aerobic 120-rpm rotating (A120) experiments were performed in a rotating incubator with a rotation amplitude of 5 cm and rotation rates of 80 rpm and 120 rpm, respectively. No atmospheric control was imposed for the static and rotating incubators.

Cell cultures were sampled at 0 h, 8 h, 16 h, 20 h, 24 h, 28 h, 32 h, 36 h, 40 h and 48 h (total 10 steps) to monitor the cell growth and the dissolved oxygen concentration in the medium (DOC). The cell growth was determined by measuring the optical density at 600 nm (OD_{600}), using a spectrophotometer (Unico UV-2102-PC). At each step, one flask (not sampled before) from each group was selected to measure the DOC with a Dual-Input Multi-parameter Meter (HQ40d, Hach Company, the sensitivity is 0.01 mg/l). The time-course experiments were repeated for three times to test reproducibility of results. Similar trends of the cell growth and oxygen consumption were observed in the three repeated experiments.

To examine the properties of magnetosomes, in this study, whole cells of 48 h were harvested by centrifugation of $\sim$2.5 liters of cultures for each growth group with an Eppendorf 5810R centrifuge at 10,000 rpm for 10 min at 4°C. To avoid oxidation, all sample loading, cell drying and magnetosome isolation were carried out inside an anaerobic glove box. Cell samples from each growth group were divided into three parts: (1) $\sim 10^{10}$ cells were loaded into a non-magnetic gelatin capsule for magnetic measurement; (2) $\sim 10^{11}$ cells were dried at room temperature for XRD analysis; and (3) $\sim 10^{10}$ cells were used for isolating magnetosomes. To isolate magnetosomes, cells were resuspended in $\sim$50 ml of distilled water, disrupted by an ultrasonicator (VCX130, SONICS, U.S.A) at 0°C; magnetosomes were collected magnetically with a bar magnet, and then washed with distilled water at least five times by repeated dispersion using a sonicator. All samples were packed in small plastic screw tubes with nitrogen protection and then were stored at -20°C in a refrigerator prior to measurements. Because all samples were prepared and measured using the same procedure, differences caused by sample preparation and measurements can be excluded; therefore, observed differences can be regarded as growth effects.

In addition, anaerobic 120-rpm rotating (AN120) cultures in a rotation incubator were performed in order to further test the rotating effects on magnetite magnetosome formation. TEM, hysteresis loops and FORC measurements on 48-h grown cells were conducted. Data were compared with the results of ANS cultures.

Magnetic Measurements

Room-temperature magnetic measurements of whole cell samples, including hysteresis loops and first-order reversal curves (FORCs), were performed on an Alternating Gradient Force Magnetometer (Model MicroMag 2900, Princeton Measurements Corporation, sensitivity is 1.0×10^{-11} Am^2). Hysteresis loops were measured between $\pm$ 500 mT. Saturation magnetization (M_s), saturation remanence (M_{rs}) and coercivity (B_c) were determined after correcting for linear contributions from diamagnetic and paramagnetic phases. Remanence coercivity (B_{cr}) was determined from a back-field demagnetization curve. FORCs were measured following the protocol described by Roberts et al. (2000). FORC diagrams were calculated using the FORCinel v1.18 software with a smoothing factor of 2 (Harrison and Feinberg 2008).

Low-temperature magnetic measurements of whole cell samples were performed on a Quantum Design Magnetic Property Measurement System (MPMS XP-5). Zero-field cooled (ZFC) curves were obtained by cooling the samples from 300 K to 5 K in zero magnetic field. Then, the samples were given a saturation remanence in a 2.5-T field (hereafter termed as $SIRM_{5K\_2.5T}$) and the remanence was measured during warming to 300 K in zero field. The field-cooled (FC) curves were obtained by cooling the samples from 300 K to 5 K in a 2.5-T field. Then, a $SIRM_{5K\_2.5T}$ was imparted and the remanence was measured during warming to 300 K in zero field. The Verwey transition temperature (T_v) was defined as the temperature of the maximum of the first derivative of the FC curves. The δ ratio (δ_{FC}/δ_{ZFC}) was calculated after Moskowitz et al. (1993).

XRD Analyses

XRD analyses of whole cell samples were performed on a DMAX2400 X-ray diffractometer using Cu K_α radiation at 40 kV and 80 mA, step-scan mode (0.02° intervals) with the sampling time of 6 s at each step. The wavelength of Gu/K-α (1.54056 Å) was used to calculate d-space values. Using the Bragg equation for cubic systems, the lattice cell parameter a_0 was determined by the Nelson-Riley Extrapolation method (Nelson and Riley 1945).

TEM Analyses

Conventional TEM observations of whole cells were performed on an FEI Tecnai-20 TEM with an acceleration voltage of 120 kV. Magnetosome dimensions were measured from the TEM images along the long axis (length, L) and width perpendicular to the long axis (W) with the Adobe Photoshop CS software. The grain size (S) was defined as (L+W)/2, and the shape factor was defined as W/L of magnetosomes. High resolution TEM (HRTEM) observations of isolated magnetosomes were conducted on a JEM-2010 TEM with an accelerating voltage of 200 kV. Digital Micrograph software was used for image processing (filtering of HRTEM images and obtaining Fast Fourier transform (FFT) patterns). Given a face center cubic (fcc) structure for magnetite, the ideal morphology of magnetosomes was reconstructed based on HRTEM and the corresponding FFT images of individual particles (Faivre et al. 2008). Selected area electron diffraction (SAED) patterns were recorded from a group of magnetosomes at various camera lengths.

RESULTS

Cell Growth, Oxygen Consumption and Magnetosome Formation

As shown in Figure 1a, the AMB-1 cells undergo a comparable trend of cell growth under four different growth conditions, ANS, AS, A80 and A120. The number of cells increases slowly during a lag phase from 0−16 h, it then increases rapidly during an exponential phase from 16−32 h, and remains nearly constant or decreases slightly during a stationary phase from 32−48 h. However, the cell growth densities between the four groups differ significantly. At any given culture time, the cell growth density was consistently ANS < AS < A80 < A120.

Initial DOC values were 0.07 mg/l, 5.03 mg/l, 6.98 mg/l and 7.89 mg/l for the ANS, AS, A80 and A120 cultures, respectively, which suggests that the oxygen supply was greatest in the A120 growth condition. The dissolved oxygen in cultures was consumed by cell respiration during cell growth, as a result, the DOC decreased rapidly (Figure 1b). After 32 h of cultivation, the DOC in the AS, A80 and A120 media were below detectable levels, indicating that the external oxygen supply from the air could not keep pace with the oxygen consumption of the AMB-1 cell respiration. After 48 h cultivation, all four growth media have more than 5 μM of dissolved iron remaining in the medium. This indicates that all cells grew in iron rich rather than iron-starving conditions.

For the ANS, AS, A80 and A120 cultures, the magnetosomes were first detectable in cells at 8 h, 20 h, 24 h and 28 h, respectively, which corresponds to DOC values of about 0.00 mg/l, 0.44 mg/l, 0.45 mg/l and 0.20 mg/l, respectively. This indicates that AMB-1 started to synthesize magnetosomes only in a lower DOC level (e.g., $\leq$ 0.45 mg/l at 26°C). This observation is consistent with previous findings that moderate to high oxygen levels can inhibit the formation of magnetite, and that magnetosomes are synthesized by AMB-1 only under microaerobic to anaerobic conditions (Yang et al. 2001).

Temporal variations of OD_{600}, average magnetosome numbers per cell, and mean grain sizes indicate that the magnetosomes are formed dominantly during the exponential growth phase (Figures 1a, c, d). Based on this, the 48 h-grown cells were harvested and comparatively analyzed to investigate the effects of growth conditions on the synthesized magnetosomes. As expected, XRD analyses on the whole cell samples indicate that magnetites were synthesized by the AMB-1 cells grown under the four different conditions. Based on XRD spectrum, the lattice parameter values calculated are 8.403 Å, 8.403 Å, 8.408 Å and 8.402 Å for the ANS, AS, A80 and A120 magnetites, respectively.

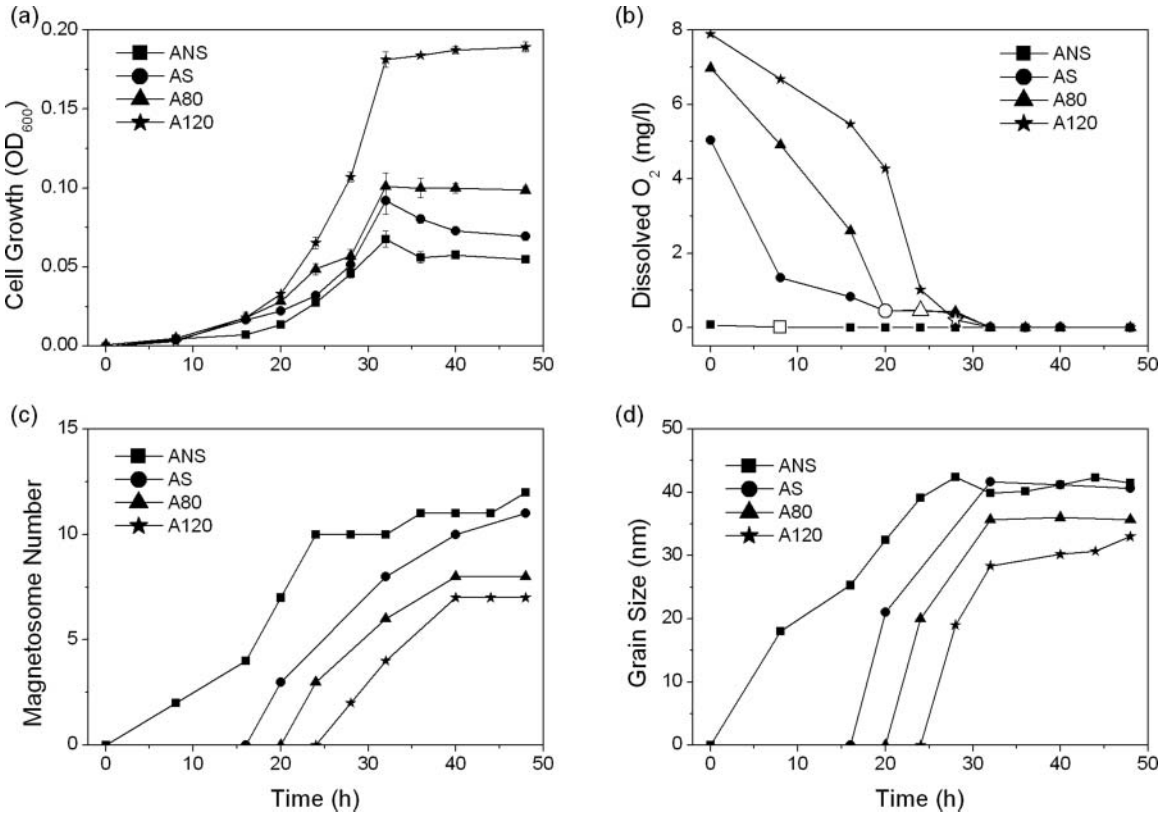

FIG. 1. (a) Temporal variations of cell growth (OD_{600}) (a), oxygen concentration (dissolved oxygen concentration, DOC) (b), average magnetosome number per cell (c) and mean grain size (d). The solid square, cycle, triangle and star lines indicate the anaerobic static (ANS), aerobic static (AS), aerobic 80-rpm rotating (A80) and aerobic 120-rpm rotating (A120) cultures, respectively. The open symbols on the DOC curves indicate the time points at which the magnetosomes are first detectable within AMB-1 cells.

Characteristics of Magnetosomes

From the ANS to A120 growth conditions, the cells produced fewer magnetosomes with decreasing grain sizes (Figures 1c, d and 2). The average numbers of magnetosomes per cell of AMB-1 were 12 ± 5, 11 ± 5, 8 ± 3 and 7 ± 4 for the ANS, AS, A80 and A120 cultures, respectively, with average grain sizes of 41.5 ± 15.0 nm, 40.6 ± 14.7 nm, 35.7 ± 12.3 nm and 33.0 ± 8.5 nm, respectively. The grain size distribution of magnetosomes is negatively skewed and relatively wide for the ANS and AS cultures, while it is nearly normal distributed and narrow for the A80 and A120 cultures. The average values of shape factor of magnetosomes determined from TEM images are 0.78, 0.79, 0.85 and 0.89 for the ANS, AS, A80 and A120 cultures, respectively (Figure 2), which indicates a change in crystal shape from more elongated to cubic-like.

TEM observations indicate that the AMB-1 cells grown under the four different conditions commonly produce 5–20 magnetosomes arranged into a linear fragmental chain in each cell (Figure 3). Interestingly, HRTEM observations indicate that the frequency of twinned crystals for ANS, AS, A80 and A120 cultures are approximately 20.2% (of 649 particles), 21.9% (of 593 particles), 33.8% (of 500 particles) and 51.6% (of 629 particles), respectively. Multiple twins in the magnetosomes were occasionally observed in the A120 culture (Figure 3d).

Both SAED and HRTEM analyses on isolated magnetosomes confirm that the magnetosomes formed by AMB-1 cells are solely magnetite (Figures 3 and 4). Representative HRTEM images of mature magnetosomes recorded from [011] zone axis of magnetite and the corresponding models are shown in Figure 4. The surface faces at the edges for the four types of magnetosomes are identical and can be identified as $\{111\}$ and $\{100\}$ faces. This indicates that the magnetite magnetosomes formed by AMB-1 under the four different conditions have a same crystal habit of truncated octahedron.

FORC Diagrams and Hysteresis Parameters

The FORC distributions indicate a dominant SD signal for the ANS and AS magnetite magnetosomes, and a mixture of SD and superparamagnetic (SP) for the A80 and A120 magnetite magnetosomes. The narrow vertical spread indicates weak or negligible inter-chain or inter-cell magnetostatic interactions. Nevertheless, the horizontal spread of the FORC distribution, which indicates the microcoercivity distributions of magnetic minerals, differs and contracts towards lower values from the

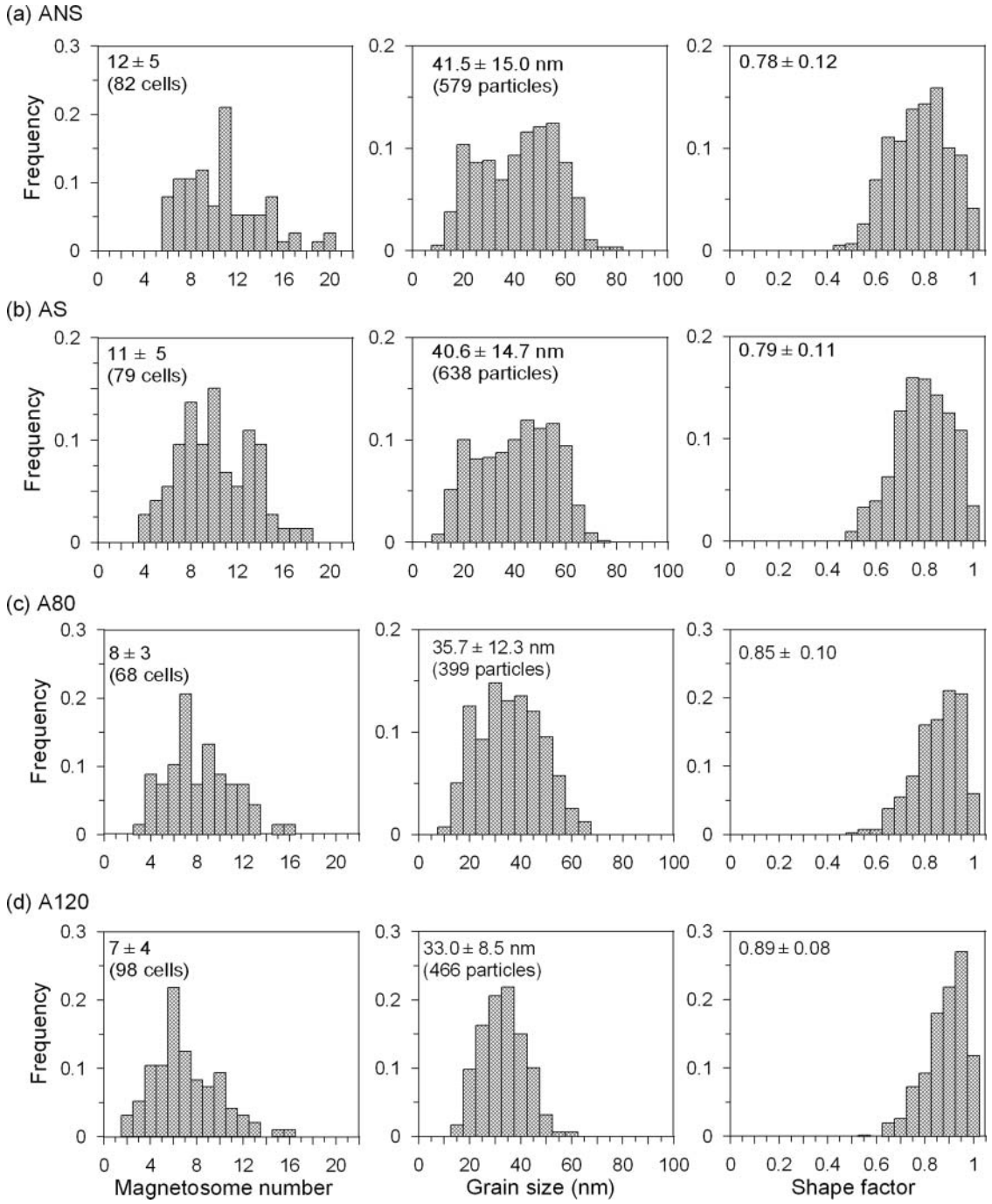

FIG. 2. Histograms of crystal number (*left*), grain size (*middle*), and shape factor (*right*) of magnetite magnetosomes synthesized by the AMB-1 cells after 48 h cultivation. (a) Anaerobic static culture (ANS). (b) Aerobic static culture (AS). (c) Aerobic 80-rpm rotating culture (A80). (d) Aerobic 120-rpm rotating culture (A120).

ANS to the A120 cells (Figure 5). The peak coercivity ($H_{c,\,FORC}$) is approximately 30.6 mT, 20.8 mT, 13.9 mT and 4.6 mT for the ANS, AS, A80 and A120 cells, respectively. The hysteresis parameters B_c, B_{cr}, and M_{rs}/M_s gradually decrease from the ANS to A120 cultures, e.g., $B_c = 22.0$ mT, $B_{cr} = 31.3$ mT and $M_{rs}/M_s = 0.45$ for the ANS cells and $B_c = 5.2$ mT, $B_{cr} = 9.3$ mT and $M_{rs}/M_s = 0.31$ for the A120 cells (Table 1). The systematic decreasing of magnetic parameters can be interpreted as a result of decreasing of grain size and crystal elongation, and increasing of crystal twinning frequencies in the magnetite magnetosomes.

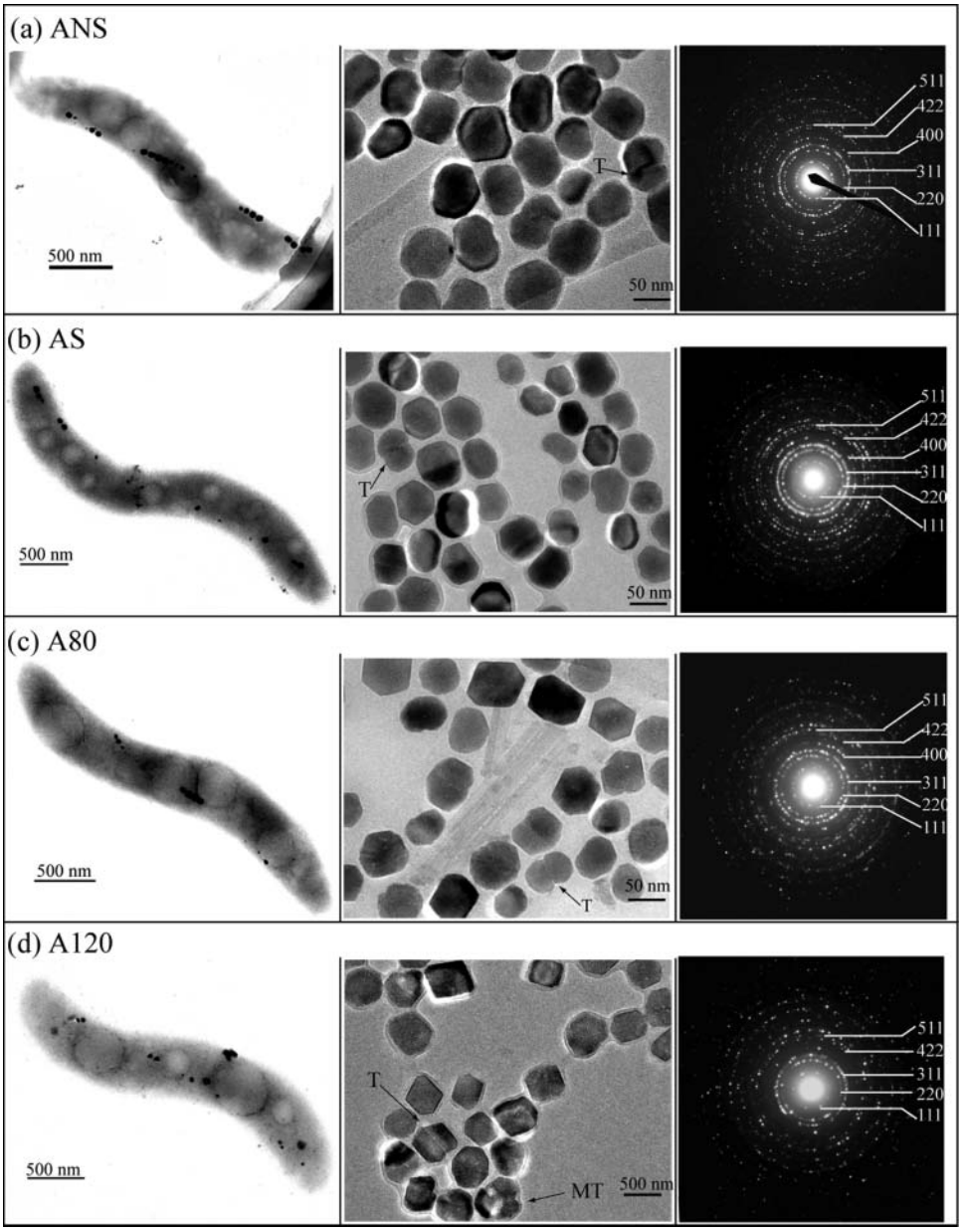

FIG. 3. Features of magnetite magnetosomes formed by the AMB-1 cells grown under the four different conditions after 48 h cultivation. (a) Anaerobic static culture (ANS). (b) Aerobic static culture (AS). (c) Aerobic 80-rpm rotating culture (A80). (d) Aerobic 120-rpm rotating culture (A120). From left to right, the first column contains typical TEM images of intact AMB-1 cells, the second column contains typical TEM images of isolated magnetosomes, and the third column contains selected area electron diffraction (SAED) patterns recorded from a group of isolated magnetosomes. 'T' and 'MT' indicate twinned and multiple-twinned crystals, respectively. TEM observations indicate that the AMB-1 cells grown under all four conditions form a similar fragmental chain of magnetosomes, but with significant differences in crystal size, morphology and twinning frequency. The analyses of SAED patterns and *d*-spacing values confirm that all four types of magnetosomes are composed solely of magnetite.

The Verwey Transition

T_v systematically decreases with growth conditions, i.e., 108 K, 106 K, 104 K and 98 K for the ANS, AS, A80 and A120 cells, respectively. The sharpness of Verwey transition behavior (i.e., the peak magnitude of dM/dT) similarly decreases (Figure 5). The observed reduction of T_v and sharpness of the Verwey transition from the ANS to A120 cultures indicates that the degree of non-stoichiometry of magnetite in the magnetosomes increases with increasing of oxygen availability. Additionally, the remanence in the high-temperature interval ($T > T_v$, e.g., 120–300 K) decreased continuously for the A80 and A120 cells is associated with a gradual unblocking of SP particles. As seen in Table 1, the reduced δ ratio (δ_{FC}/δ_{ZFC}) value for the A120 cells, which is lower than the threshold value of

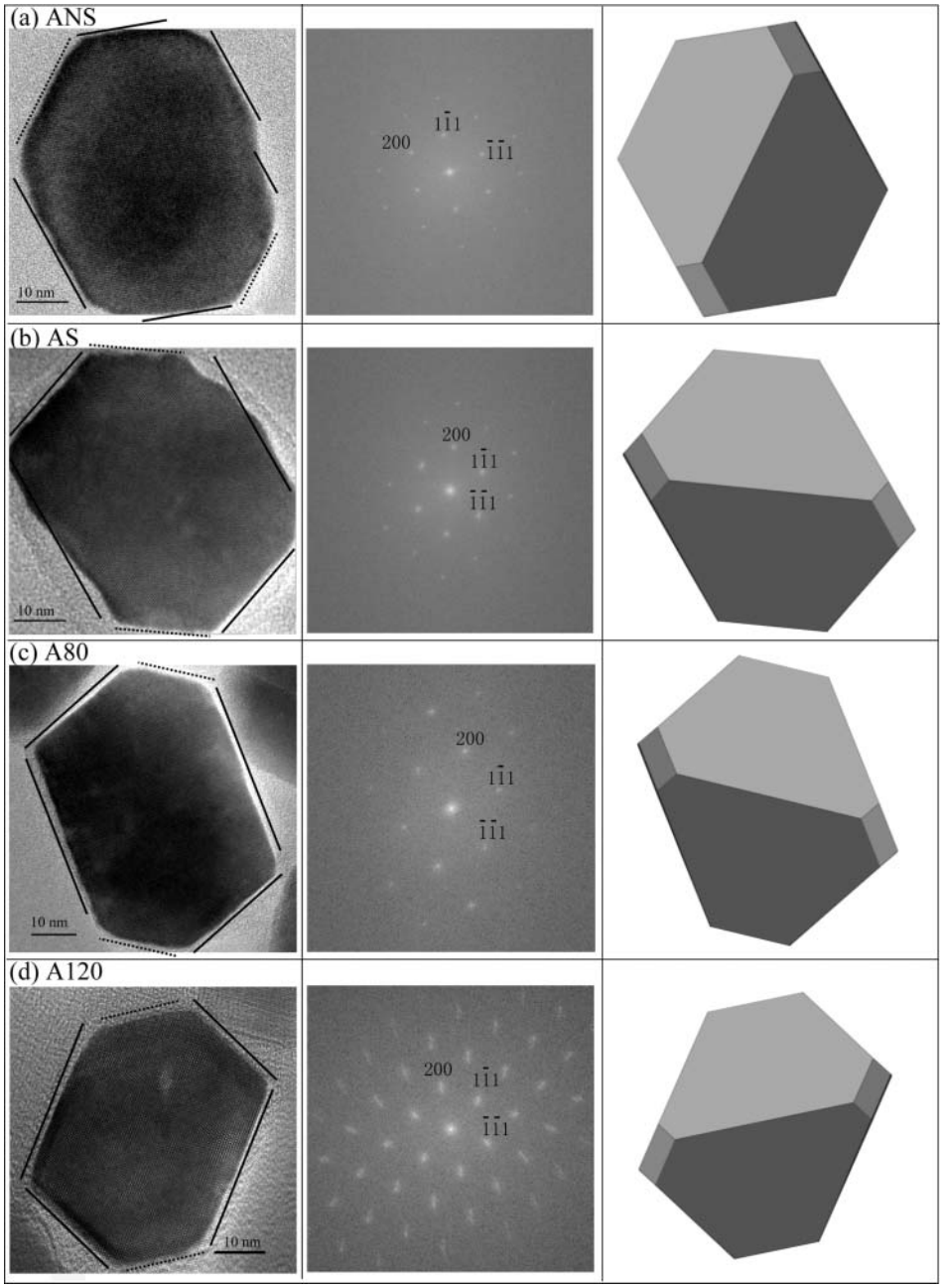

FIG. 4. HRTEM images of individual magnetite magnetosomes recorded along the [011] zone axis of magnetite (*left*), and their corresponding Fast Fourier transform (FFT) images (*middle*) and morphological models (*right*). (a) Anaerobic static culture (ANS). (b) Aerobic static culture (AS). (c) Aerobic 80-rpm rotating culture (A80). (d) Aerobic 120-rpm rotating culture (A120). On the left column, solid lines and dash lines indicates {111} and {100} faces, respectively. On the right column, corresponding model are oriented with respect to crystal direction deduced from FFT analysis. HRTEM imaging, FFT analyzing and morphological modeling show that there is no significant difference in crystal habits between four types of magnetite magnetosomes.

2.0 for the Moskowitz test, may be related to the presence of a high-fraction of SP particles and poor chain configuration (Moskowitz et al. 1993; Moskowitz et al. 2008; Li et al. 2009).

The Rotating Effect

The time courses of cell growth are not distinguishable between the ANS and AN120 cultures (Figure 6a). TEM observations of grain sizes and shapes of magnetite magnetosomes (data not shown), hysteresis loop and FORC diagrams of 48 h-grown cells demonstrated that the difference of magnetite magnetosomes synthesized in AN120 and ANS cultures is weak and negligible (Figure 6b–d). This indicates that the rotating, at least up to 120 rpm, does not significantly affect the magnetite magnetosome formation. Therefore, we inferred that the

TABLE 1
Magnetic parameters of the bulk samples of AMB-1 cells after 48 h growth

Culture	B_{cr} (mT)	B_c (mT)	B_{cr}/B_c	M_{rs}/M_s	T_v (K)	δ_{FC}	δ_{ZFC}	δ_{FC}/δ_{ZFC}
ANS	31.3	22.0	1.42	0.45	108	0.395	0.166	2.38
AS	22.0	16.1	1.37	0.44	106	0.353	0.116	3.05
A80	16.8	10.6	1.59	0.38	104	0.369	0.133	2.77
A120	9.3	5.2	1.80	0.31	98	0.472	0.295	1.60

Notes: The ANS, AS, A80 and A120 indicate anaerobic static, aerobic static, aerobic 80-rpm rotating and aerobic 120-rpm rotating cultures, respectively. The B_{cr}, B_c, M_{rs} and M_s indicate remanence coercivity, coercivity, saturation remanence and saturation magnetization, respectively. The T_v indicates the Verwey transition temperature defined as the temperature for the maximum of the first derivative of the FC curves. The δ_{FC} and δ_{ZFC} are defined after Moskowitz *et al.* (1993), i.e., $\delta = (M_{80K} - M_{150K})/M_{80K}$ (M_{80K} and M_{150K} are the remanences measured at 80 K and 150 K, respectively).

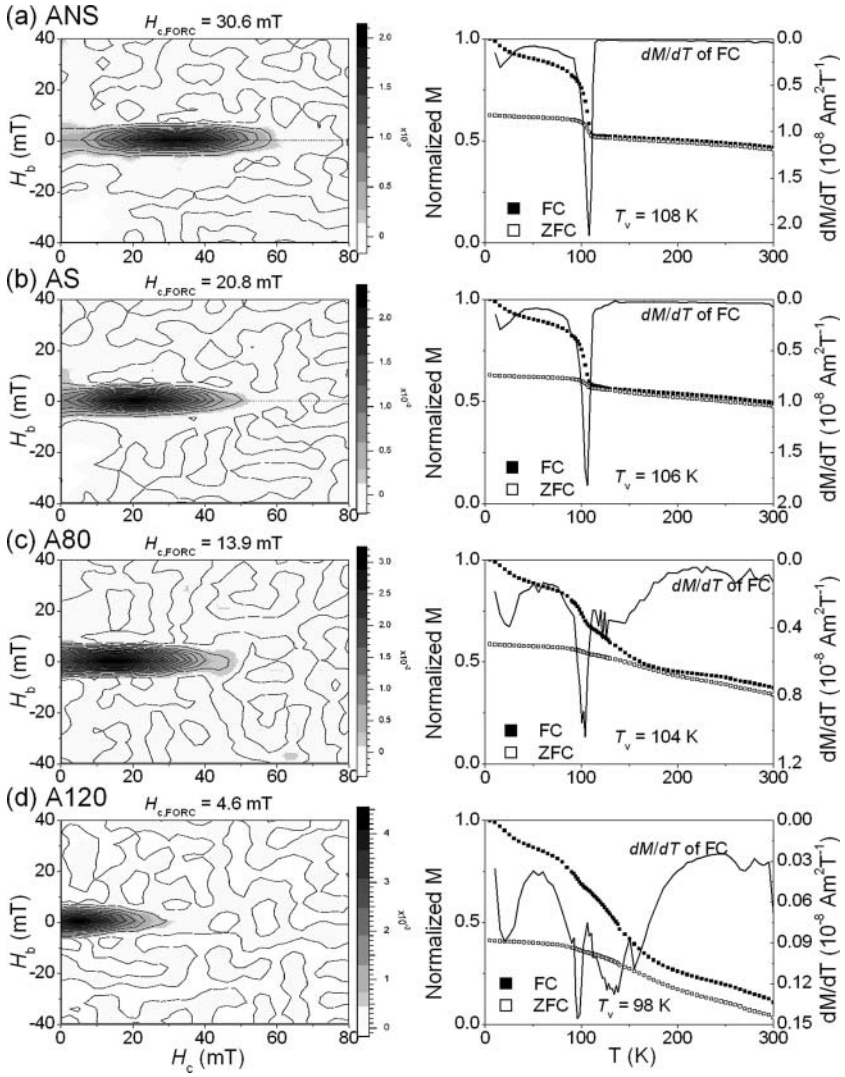

FIG. 5. Room-temperature FORC diagrams (*left*) and low-temperature magnetic properties (*right*) for the bulk sample of AMB-1 cells after 48 h cultivation. (a) Anaerobic static culture(ANS). (b) Aerobic static culture (AS). (c) Aerobic 80-rpm rotating culture (A80). (d) Aerobic 120-rpm rotating culture (A120). The FORC diagrams were calculated with a smooth factor of 2. The peak coercivity, $H_{c,FORC}$, is defined as the H_c field corresponding to the peak of the FORC distribution. Zero-field-cooled (ZFC) and field-cooled (FC) curves were used after normalizing by FC-SIRM$_{5K_2.5T}$.

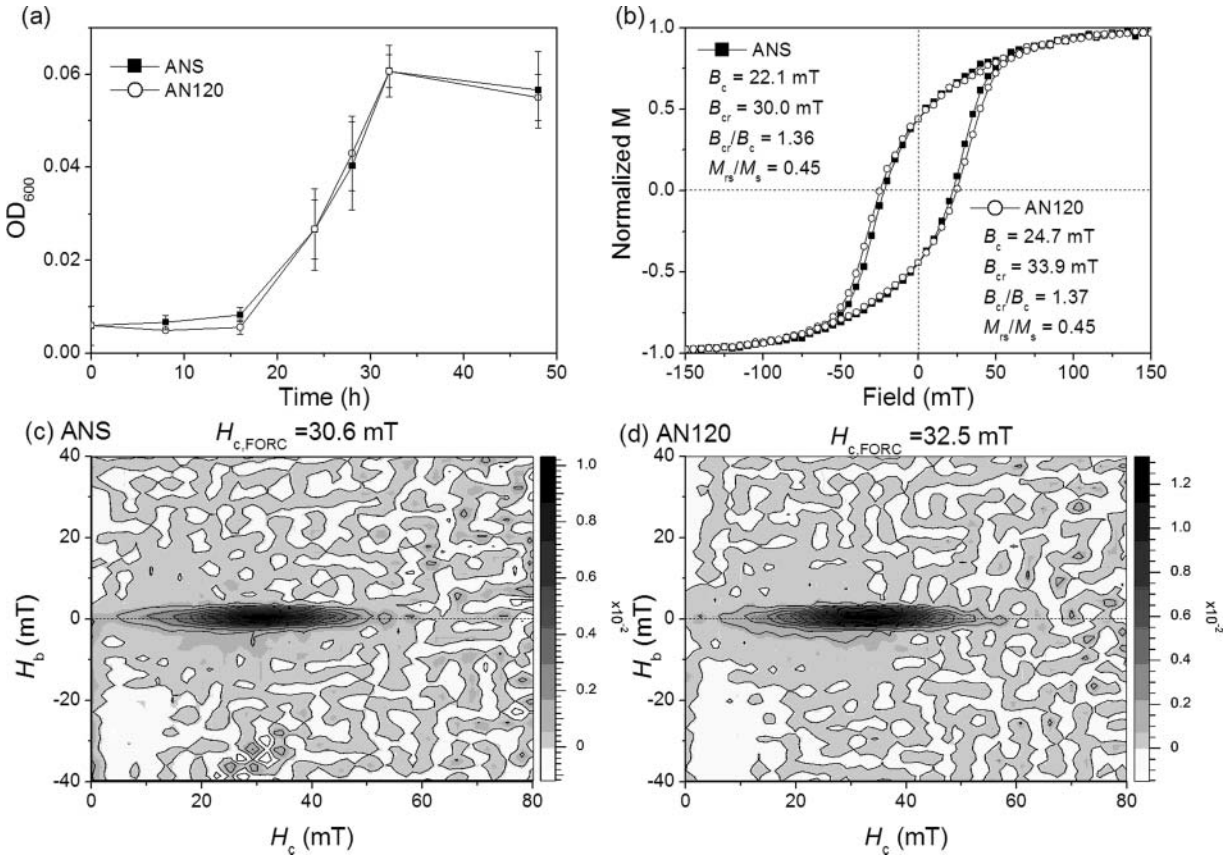

FIG. 6. Comparison of anaerobic static (ANS) (solid square line) and anaerobic 120-rpm rotating (AN120) (open cycle line) cultures. (a) Cell growth curves. (b) Hysteresis loops. (c) and (d) FORC diagrams.

possibility of above mentioned difference of magnetite magnetosomes in AMB-1 from the ANS to A120 cultures derived from the rotating influence could be precluded.

DISCUSSION

The Role of Environmental Oxygen and Rotating

In this study, the ANS growth condition can be regarded as a true anaerobic environment, while the AS, A80 and A120 growth conditions have free exchange with air and each culture thus has a constant oxygen supply to the medium. As seen from the initial DOC values (Figure 1b), the oxygen supply was increased from AS to A120. However, the external supply of oxygen could not keep pace with the consumption by growing cells. In other words, the magnetite magnetosomes in the AS, A80 and A120 cultures were formed under a similar microaerobic and anaerobic environment, but a different condition of oxygen supply in the medium.

Due to the usage of flasks rather than a bioreactor, it is hard to precisely determine the oxygen content of the growth cultures of this study. However, based on TEM analyses, AMB-1 cells started to synthesize visible magnetosomes by 8 h, 20 h, 24 h and 28 h cultivation in the ANS, AS, A80 and A120 cultures, respectively; the magnetite magnetosomes synthesized become more cube-like with smaller grain sizes, and more imperfect crystals (e.g., twinning; Figures 2 and 3). This observation confirms previous findings that environmental factors affect the physical properties of magnetite magnetosomes (Blakemore et al. 1985; Heyen and Schüler 2003; Faivre et al. 2008; Popa et al. 2009; Yang et al. 2001). These changes in magnetite magnetosome are well characterized by the changes in magnetic properties and the corresponding parameters, i.e., the B_c, B_{cr}, M_{rs}/M_s and $H_{c,FORC}$ and T_v for the samples of whole cells systematically decrease from the ANS to A120 cultures. Although the AMB-1 produced magnetite with similar grain sizes and shape factors under ANS and AS growth conditions, there is a 2 K decrease of T_v and a 27% decrease of coercivity for the latter. This reduction suggests that oxygen does play a role in the biomineralization of magnetite magnetosomes.

M. magneticum strain AMB-1 is a facultative anaerobic MTB. When it grows aerobically, cells of AMB-1 prefer to use O_2 as the terminal electron acceptor (TEA) (Matsunaga et al. 2005; Yang et al. 2001). When it grows anaerobically and nitrate is available in culture, it can use nitrate as TEA (Matsunaga et al. 1991; Matsunaga and Tsujimura 1993). This study revealed that the magnetite magnetosomes start to be

formed at different stages in four growth conditions when the DOC is lower than a threshold value of ~0.45 mg/l, which could correspond to a switch from O_2 to nitrate TEA. Bazylinski and Blakemore (1983) found that MS-1 cells grown under microaerobic condition start to extensively utilize nitrate when O_2 steadily decrease to a level of lower than ~200 μM. A similar switch could occur in AMB-1 as well. It is worth studying how magnetite magnetosome synthesis is affected during this switch in future work.

Oxygen could serve as a regulatory signal for adjusting the expression or/and activity of specific genes and proteins that are involved in controlling grain size, crystal shape, chain arrangement and crystallization of magnetite, as well as in regulating the physical and chemical conditions of magnetosome vesicles (e.g., iron supply direction, pH and redox potential), and consequently, affect the magnetite magnetosome biomineralization (Ding et al. 2010; Faivre and Schüler 2008; Murat et al. 2010; Sakaguchi et al. 1993; Scheffel et al. 2008; Short and Blakemore 1989). Overall, there needs to be a combined investigation linking the mineralization processes with the molecular processes to unravel the BCM mechanism of magnetite magnetosomes.

Another factor to be considered in the present study is the rotating effect on the magnetite synthesis. Our additional studies of ANS and AN120 cultures indicate that the rotating, at least up to 120 rpm, does not affect the cell growth in anaerobic cultures. Although there are slight increases of B_c (2.6 mT) and B_{cr} (3.9 mT) for the AN120 cells, compared with the ANS cells, their ratios of M_{rs}/M_s and B_{cr}/B_c are nearly unchanged, indicating that the rotating does not significantly influence the magnetite synthesis in AMB-1. These changes, however, clearly contrast to distinct reductions of B_c (10.9 mT), B_{cr} (12.7 mT) and M_{rs}/M_s (~30%) and an increasing of B_{cr}/B_c (~24%) for A120, compared with AS, where flakes have free contact with air (Table 1). Therefore, we infer from above observations that the environmental oxygen, instead of rotating flasks, dominantly influence the magnetite magnetosome formation in AMB-1.

The Biologically Controlled Mineralization

Molecular studies have well demonstrated that magnetite magnetosomes are formed in a stepwise manner, in which magnetosome membrane biogenesis, iron uptake, nucleation and growth of magnetite crystal, and chain arrangement are performed under strict biochemical and genetic controls (Komeili et al. 2004, 2006; Murat et al. 2010). This study demonstrated that synthesized magnetosomal magnetite, as evidenced by both TEM and magnetism, can be influenced by environmental factors (e.g., oxygen). Decreasing T_v from 108 K to 98 K from ANS to A120 implies that the synthesized magnetosomes become more non-stoichiometric magnetite (Muxworthy and McClelland 2000). The new observation casts some doubts on previous thoughts that MTB produce stoichiometric magnetite.

However, the cause for reduced T_v, which was observed for different strains of MTB and samples processed by different methods, e.g., freeze-dried cells, fresh wet cells and isolated magnetite magnetosomes, is intensively debated (Li et al. 2009, 2010a, 2010b; Moskowitz et al. 1993, 2008; Pan et al. 2005b; Prozorov et al. 2007). The reduced T_v of MTB-produced magnetite was usually interpreted as a result of oxidation of magnetosomes (Moskowitz et al. 1993; Özdemir and Dunlop 2010; Pan et al. 2005b; Weiss et al. 2004), or an intrinsic property of magnetosomal magnetites (Fischer et al. 2008; Moskowitz et al. 2008; Pan et al. 2005b). In this study, all samples were prepared under anaerobic atmosphere, and were measured in the same fashion.

We prefer to interpret the gradually decrease of T_v from the ANS to A120 cultures as a result of increasing twinning and/or ion vacancies of magnetite in magnetosomes, due to increasing oxygen supply during cell growth. The results of XRD and SAED analyses also show no maghemitization for our samples, although a slight degree of maghemitization could not be detected by these methods. Nanoscale probing on the crystal structure and composition of magnetite magnetosomes are needed in the future by using advanced TEM techniques (e.g., electron energy-loss spectroscopy) and synchrotron radiation based techniques (e.g., X-ray magnetic circular dichroism).

Geological Implications

The experimental results of AMB-1 growth in this study provide some useful clues for the bacterial mineralization in natural environments. In modern natural habitats, MTB are usually found in the highest numbers at, or just below, the oxic-anoxic interface within aquatic environments (Bazylinski et al. 2000; Simmons et al. 2004). Several recent studies have demonstrated that the oxygen concentration gradient, salinity, nitrate and temperature can strongly influence the number and composition of MTB communities (Jogler et al. 2010; Lin and Pan 2010; Simmons et al. 2004). Magnetofossils have been used as paleoenvironmental indicators from a variety of marine and freshwater sediments (Kopp and Kirschvink 2008).

It has been shown that the concentrations of magnetofossils, as well as their morphology assemblage, vary with climate oscillations (Hesse 1994; Kopp et al. 2009; Paasche and Larsen 2010; Yamazaki and Kawahata 1998). Hesse (1994) found that the cyclic variation pattern of bacterial magnetofossil concentration in the Tasman Basain in southwest Pacific Ocean sediments correlates to climatic changes. The intervals of low bacterial magnetite concentration, occurring in glacial periods, are accompanied by a change of the bacterial magnetite morphology assemblage interpreted as recording a change in bacterial species assemblage. Yamazaki and Kawahata (1998) also found that isotropic crystal magnetofossils occur in relatively oxidized conditions, while anisotropic crystal magnetofossils predominate in more reduced conditions in Pacific deep-sea sediments.

The present study revealed for the first time that, the crystal properties (e.g., number, shape factor, size and crystallinity) and associated magnetic properties (e.g., B_c, B_{cr} and T_v) of magnetite magnetosomes synthesized by AMB-1 are environmentally dependent, although it produced solely magnetite with a truncated

octahedron under different growth conditions. This suggests that physical features and magnetic properties of magnetosomes or magnetofossils could provide additional information of the bacterial growth conditions. Therefore, the reconstruction of paleoenvironment through detailed studies of the concentration, morphology assemblage and magnetic traits of magnetofossils is prospective.

CONCLUSIONS

The magnetosomes synthesized by the AMB-1 cells grown under different oxygen concentrations contained solely magnetite with a truncated octahedron, which suggests that the mineral phase and crystallographic habit of magnetosomes are strain-specific and under genetic control. However, lines of evidence presented in this study suggest that biomineralization of magnetite magnetosomes in AMB-1 can be influenced by growth conditions such as environmental oxygen concentrations. Increasing oxygen supply may result in the production of more non-stoichiometric magnetite in magnetosomes.

REFERENCES

Bazylinski DA, Blakemore RP. 1983. Denitrification and assimilatory nitrate reduction in *Aquaspirillum magnetotacticum*. Appl Environ Microbiol 46:1118–1124.

Bazylinski DA, Frankel RB, Konhauser KO. 2007. Modes of biomineralization of magnetite by microbes. Geomicrobiol J 24:465–475.

Bazylinski DA, Schlezinger DR, Howes BH, Frankel RB, Epstein SS. 2000. Occurrence and distribution of diverse populations of magnetic protists in a chemically stratified coastal salt pond. Chem Geol 169:319–328.

Blakemore RP, Short KA, Bazylinski DA, Rosenblatt C, Frankel RB. 1985. Microaerobic conditions are required for magnetite formation within *Aquaspirillum Magnetotacticum*. Geomicrobiol J 4:53–71.

Ding Y, Li JH, Liu JN, Yang J, Jiang W, Tian JS, Li Y, Pan YX, Li JL. 2010. Deletion of the *ftsZ*-Like gene results in the production of superparamagnetic magnetite magnetosomes in *Magnetospirillum gryphiswaldense*. J Bacteriol 192:1097–1105.

Edwards KJ, Bazylinski DA. 2008. Intracellular minerals and metal deposits in prokaryotes. Geobiology 6:309–317.

Faivre D, Menguy N, Pósfai M, Schüler D. 2008. Environmental parameters affect the physical properties of fast-growing magnetosomes. Am Mineral 93:463–469.

Faivre D, Schüler D. 2008. Magnetotactic bacteria and magnetosomes. Chem Rev 108:4875–4898.

Fischer H, Mastrogiacomo G, Löffler JF, Warthmann RJ, Weidler PG, Gehring AU. 2008. Ferromagnetic resonance and magnetic characteristics of intact magnetosome chains in *Magnetospirillum gryphiswaldense*. Earth Planet Sci Lett 270:200–208.

Harrison RJ, Feinberg JM. 2008. FORCinel: An improved algorithm for calculating first-order reversal curve distributions using locally weighted regression smoothing. Geochem Geophys Geosyst 9, doi:10.1029/2008GC001987.

Hesse PP. 1994. Evidence for bacterial paleoecological origin of mineral magnetic cycles in oxic and sub-oxic tasman sea sediments. Mar Geol 117:1–17.

Heyen U, Schüler D. 2003. Growth and magnetosome formation by microaerophilic *Magnetospirillum* strains in an oxygen-controlled fermentor. Appl Microbiol Biotechnol 61:536–544.

Jimenez-Lopez C, Romanek CS, Bazylinski DA. 2010. Magnetite as a prokaryotic biomarker: A review. J Geophys Res-Biogeosci 115, doi: 10.1029/2009jg001152.

Jogler C, Niebler M, Lin W, Kube M, Wanner G, Kolinko S, Stief P, Beck AJ, de Beer D, Petersen N, Pan YX, Amann R, Reinhardt R, Schüler D. 2010. Cultivation-independent characterization of *Candidatus Magnetobacterium bavaricum* via ultrastructural, geochemical, ecological and metagenomic methods. Environ Microbiol 12:2466–2478.

Komeili A, Li Z, Newman DK, Jensen GJ. 2006. Magnetosomes are cell membrane invaginations organized by the actin-like protein MamK. Science 311:242–245.

Komeili, A, Vali, H, Beveridge, TJ, Newman, DK. 2004. Magnetosome vesicles are present before magnetite formation, and MamA is required for their activation. Proc Natl Acad Sci USA 101:3839–3844.

Kopp RE, Kirschvink JL. 2008. The identification and biogeochemical interpretation of fossil magnetotactic bacteria. Earth-Sci Rev 86:42–61.

Kopp RE, Schumann D, Raub TD, Powars DS, Godfrey LV, Swanson-Hysell NL, Maloof AC, Vali H. 2009. An Appalachian Amazon? Magnetofossil evidence for the development of a tropical river-like system in the mid-Atlantic United States during the Paleocene-Eocene thermal maximum. Paleoceanography 24, doi: 10.1029/2009PA001783.

Li JH, Pan YX, Chen GJ, Liu QS, Tian LX, Lin W. 2009. Magnetite magnetosome and fragmental chain formation of *Magnetospirillum magneticum* AMB-1: Transmission electron microscopy and magnetic observations. Geophys J In 177:33–42.

Li JH, Pan YX, Liu QS, Qin HF, Deng CL, Che RC, Yang XA. 2010a. A comparative study of magnetic properties between whole cells and isolated magnetosomes of *Magnetospirillum magneticum* AMB-1. Chin Sci Bull 55:38–44.

Li JH, Pan YX, Liu Q, Yu-Zhang K, Menguy N, Che RC, Qin HF, Lin W, Wu WF, Petersen N, Yang XA. 2010b. Biomineralization, crystallography and magnetic properties of bullet-shaped magnetite magnetosomes in giant rod magnetotactic bacteria. Earth Planet Sci Lett 293:368–376.

Lin W, Pan YX. 2010. Temporal variation of magnetotactic bacterial communities in two freshwater sediment microcosms. FEMS Microbiol Lett 302:85–92.

Matsunaga T, Okamura Y, Fukuda Y, Wahyudi AT, Murase Y, Takeyama H. 2005. Complete genome sequence of the facultative anaerobic magnetotactic bacterium *Magnetospirillum* sp. strain AMB-1. DNA Res 12:157–166.

Matsunaga T, Sakaguchi T, Tadokoro F. 1991. Magnetite formation by a magnetic bacterium capable of growing aerobically. Appl Microbiol Biot 35:651–655.

Matsunaga T, Tsujimura N. 1993. Respiratory inhibitors of a magnetic bacterium *magnetospirillum* sp. AMB-1 capable of growing aerobically. Appl Microbiol Biotechnol 39:368–371.

Moskowitz BM, Bazylinski DA, Egli R, Frankel RB, Edwards KJ. 2008. Magnetic properties of marine magnetotactic bacteria in a seasonally stratified coastal pond (Salt Pond, MA, USA). Geophys J Int 174:75–92.

Moskowitz BM, Frankel RB, Bazylinski DA. 1993. Rock magnetic criteria for the detection of biogenic magnetite. Earth Planet Sci Lett 120:283–300.

Murat D, Quinlan A, Vali H, Komeili A. 2010. Comprehensive genetic dissection of the magnetosome gene island reveals the step-wise assembly of a prokaryotic organelle. Proc Natl Acad Sci USA 107:5593–5598.

Muxworthy AR, McClelland E. 2000. Review of the low-temperature magnetic properties of magnetite from a rock magnetic perspective. Geophys J Int 140: 101–114.

Nelson JB, Riley DP. 1945. An experimental investigation of extrapolation methods in the derivation of accurate unit-cell dimensions of crystals. Proc Phys Soc 57: 160–177.

Özdemir Ö, Dunlop DJ. 2010. Hallmarks of maghemitization in low-temperature remanence cycling of partially oxidized magnetite nanoparticles. J Geophys Res 115: doi: 10.1029/2009jb006756.

Paasche Ø, Larsen J. 2010. Changes in lake stratification and oxygen distribution inferred from two contrasting records of magnetotactic bacteria and diatoms. J Geophys Res-Biogeosci 115: doi: 10.1029/2009jg001081.

Pan YX, Petersen N, Davila AF, Zhang LM, Winklhofer M, Liu QS, Hanzlik M, Zhu RX. 2005a. The detection of bacterial magnetite in recent sediments of Lake Chiemsee (southern Germany). Earth Planet Sci Lett 232:109–123.

Pan YX, Petersen N, Winklhofer M, Davila AF, Liu QS, Frederichs T, Hanzlik M, Zhu RX. 2005b. Rock magnetic properties of uncultured magnetotactic bacteria. Earth Planet Sci Lett 237:311–325.

Popa R, Fang W, Nealson KH, Souza-Egipsy V, Berquo TS, Banerjee SK, Penn LR. 2009. Effect of oxidative stress on the growth of magnetic particles in *Magnetospirillum magneticum*. Int Microbiol 12:49–57.

Pósfai M, Dunin-Borkowski RE. 2009. Magnetic nanocrystals in organisms. Elements 5:235–240.

Prozorov R, Prozorov T, Williams TJ, Bazylinski DA, Mallapragada SK, Narasimhan B. 2007. Magnetic irreversibility and Verwey transition in nano-crystalline bacterial magnetite. Phys Rev B 76: doi:10.1103/physRevB1176.054406.

Roberts AP, Pike CR, Verosub KL. 2000. First-order reversal curve diagrams: A new tool for characterizing the magnetic properties of natural samples. J Geophys Res-Solid Earth 105:28461–28476.

Sakaguchi H, Hagiwara H, Fukumori Y, Tamaura Y, Funaki M, Hirose S. 1993. Oxygen concentration-dependent induction of a 140-KDa protein in magnetic bacterium *magnetospirillum magnetotacticum* MS-1. FEMS Microbiol Lett 107:169–173.

Schüler D. 2008. Genetics and cell biology of magnetosome formation in magnetotactic bacteria. FEMS Microbiol Rev 32:654–672.

Scheffel A, Gardes A, Grunberg K, Wanner G, Schüler D. 2008. The major magnetosome proteins MamGFDC are not essential for magnetite biomineralization in *Magnetospirillum gryphiswaldense* but regulate the size of magnetosome crystals. J Bacteriol 190:377–386.

Short KA, Blakemore RP. 1989. Periplasmic superoxide dismutases in *Aquaspirillum Magnetotacticum*. Arch Microbiol 152:342–346.

Simmons SL, Sievert SM, Frankel RB, Bazylinski DA, Edwards KJ. 2004. Spatiotemporal distribution of marine magnetotactic bacteria in a seasonally stratified coastal salt pond. Appl Environ Microbiol 70:6230–6239.

Weiss BP, Kim SS, Kirschvink JL, Kopp RE, Sankaran M, Kobayashi A, Komeili A. 2004. Ferromagnetic resonance and low-temperature magnetic tests for biogenic magnetite. Earth Planet Sci Lett 224:73–89.

Yamazaki T, Kawahata H. 1998. Organic carbon flux controls the morphology of magnetofossils in marine sediments. Geology 26:1064–1066.

Yang CD, Takeyama H, Tanaka T, Matsunaga T. 2001. Effects of growth medium composition, iron sources and atmospheric oxygen concentrations on production of luciferase-bacterial magnetic particle complex by a recombinant *Magnetospirillum magneticum* AMB-1. Enzyme Microb Technol 29:13–19.